

Journal of Mechanical Engineering

An International Journal

Volume 9 No. 1

July 2012

ISSN 1823-5514

-
- | | |
|--|---|
| Design Improvement of a Versatile Ducted-Fan UAV | Adnan Maqsood
Tiauw Hiong Go |
| Design and Flight Analysis of the Kenyalang-1 Fuel Cell Powered Unmanned Aircraft | Thomas A. Ward |
| Effective Data Collection and Analysis for Efficient Implementation of Standardized Work (SW) | Ahmed Jaffar
Nurul Hayati Abdul Halim
Noriah Yusoff |
| Knee Dynamic Analysis Based on 2D-to-3D Registration of Fluoroscopic and Angiographic Images | Amir Hossein Savch
Ali Reza Zali
Seyyed Morteza Kazemi
Sohrab Keyhani
Hanafiah Yussof
Hamid Reza Katouzian
Qureish Vanat
Mahmoud Chizari |
| Longitudinal Static Stability of a Blended Wing-Body Unmanned Aircraft with Canard as Longitudinal Control Surface | Rizal E. M. Nasir
Wahyu Kuntjoro
Wirachman Wisnoe |
| Modal Extraction Accuracy Using Single Station Time Domain (SSTD) Technique | A. F. Ghazali
A. A. Mat Isa |
-

JOURNAL OF MECHANICAL ENGINEERING (JMeChE)

EDITORIAL BOARD

EDITOR IN CHIEF:

Professor Wahyu Kuntjoro – Universiti
Teknologi MARA, Malaysia

EDITORIAL BOARD:

Professor Ahmed Jaffar – Universiti Teknologi
MARA, Malaysia

Professor Bodo Heimann – Leibniz University
of Hannover Germany

Dr. Yongki Go Tiauw Hiong – Nanyang
Technological University, Singapore

Professor Mirosław L Wyszynski – University
of Birmingham, UK

Professor Ahmad Kamal Ariffin Mohd Ihsan –
UKM Malaysia

Professor P. N. Rao, University of Northern
Iowa, USA

Professor Abdul Rahman Omar – Universiti
Teknologi MARA, Malaysia

Professor Masahiro Ohka – Nagoya University,
Japan

Datuk Professor Ow Chee Sheng – Universiti
Teknologi MARA, Malaysia

Professor Yongtae Do – Daegu University,
Korea

Dr. Ahmad Azlan Mat Isa – Universiti
Teknologi MARA, Malaysia

Professor Ichsan S. Putra – Bandung Institute
of Technology, Indonesia

Dr. Salmiah Kasolang – Universiti Teknologi
MARA, Malaysia

Dr. Mohd. Afian Omar – SIRIM Malaysia
Dato' Professor Mohamed Dahalan Mohamed
Ramli – Universiti Teknologi MARA,
Malaysia

Professor Darius Gnanaraj Solomon – Karunya
University, India

Professor Mohamad Nor Berhan – Universiti
Teknologi MARA, Malaysia

Professor Bernd Schwarze – University of
Applied Science, Osnabrueck, Germany

Dr. Rahim Atan – Universiti Teknologi
MARA, Malaysia

Professor Wirachman Wisnoe – Universiti
Teknologi MARA, Malaysia

Dr. Thomas Ward – Universiti Teknologi
MARA, Malaysia

Dr. Faqir Gul – Institute Technology Brunei,
Brunei Darussalam

Dr. Valliyappan David a/l Natarajan –
Universiti Teknologi MARA, Malaysia

EDITORIAL EXECUTIVE:

Dr. Koay Mei Hyie
Rosnadiyah Bahsan
Farrahshaida Mohd. Salleh
Mohamad Mazwan Mahat

© UiTM Press, UiTM 2012

All rights reserved. No part of this publication may be reproduced, copied, stored in any retrieval system or transmitted in any form or by any means; electronic, mechanical, photocopying, recording or otherwise; without prior permission in writing from the Director of UiTM Press, Universiti Teknologi MARA, 40450 Shah Alam, Selangor Darul Ehsan, Malaysia. e-mail: penerbit@salam.uitm.edu.my

Journal of Mechanical Engineering (ISSN 1823-5514) is published by the Faculty of Mechanical Engineering (FKM) and UiTM Press, Universiti Teknologi MARA, 40450 Shah Alam, Selangor, Malaysia.

The views, opinions and technical recommendations expressed herein are those of individual researchers and authors and do not necessarily reflect the views of the Faculty or the University.

Journal of Mechanical Engineering

An International Journal

Volume 9 No. 1

July 2012

ISSN 1823-5514

1. Design Improvement of a Versatile Ducted-Fan UAV 1
Adnan Maqsood
Tiauw Hiong Go

2. Design and Flight Analysis of the Kenyalang-1 Fuel Cell Powered Unmanned Aircraft 19
Thomas A. Ward

3. Effective Data Collection and Analysis for Efficient Implementation of Standardized Work (SW) 45
Ahmed Jaffar
Nurul Hayati Abdul Halim
Noriah Yusoff

4. Knee Dynamic Analysis Based on 2D-to-3D Registration of Fluoroscopic and Angiographic Images 79
Amir Hossein Saveh
Ali Reza Zali
Seyyed Morteza Kazemi
Sohrab Keyhani
Hanafiah Yusoff
Hamid Reza Katouzian
Qureish Vanat
Mahmoud Chizari

5. Longitudinal Static Stability of a Blended Wing-Body Unmanned Aircraft with Canard as Longitudinal Control Surface 99
Rizal E. M. Nasir
Wahyu Kuntjoro
Wirachman Wisnoe
6. Modal Extraction Accuracy Using Single Station Time Domain (SSTD) Technique 123
A. F. Ghazali
A. A. Mat Isa

Design Improvement of a Versatile Ducted-Fan UAV

Adnan Maqsood

*Research Centre for Modeling and Simulation
National University of Science and Technology, H-12
Islamabad 44000, Islamic Republic of Pakistan*

Tiauw Hiong Go

*School of Mechanical and Aerospace Engineering
Nanyang Technological University, Singapore 639798
Republic of Singapore*

ABSTRACT

The paper discusses the aerodynamic design improvement of a ducted fan Unmanned Aerial Vehicle (UAV). The UAV is capable of take-off vertically, hover and transition to cruise and is equipped with wings. The aerodynamics of the UAV is estimated through wind-tunnel experiments. The design improvement is carried out for the two phases of mission profile: hover and cruise. During hover flight, modifications in propulsion system and consequent effects on the controllability of the platform are investigated. The existing single propeller motor is replaced with contra-rotating propulsion system. Moreover, control surface positioning is also refined. During forward flight condition, the aerodynamic forces and moment is evaluated for plain ducted-fan configuration. It is observed that the modified configuration has the desired flight characteristics in cruise mode as well. The improvement in the aerodynamic performance with wings of different aspect ratios is also mapped out. The improvement in lift characteristics is observed with the increase in aspect ratio.

Keywords: *Unmanned Ducted-Fan; UAV; Wind-Tunnel Testing*

Introduction

The requirement for multi-dimensional mission profiles including reconnaissance in the cluttered/urban terrains and tight space environments have paved the

way to combine the hover-capable rotorcraft technology with high speed and endurance capable fixed-wing technology. This challenging flight envelope has given birth to a very agile type of aircraft known as ‘convertible’ platforms that couple hover capability with efficient flight during forward cruise. A possible solution from the technology protagonists is the ducted-fan configuration. Ducted-fan configuration combines the advantages of both the fixed-wing and rotary wing. It possesses both the cruising ability and long flight time of the fixed wing, as well as the manoeuvrability and hovering ability of the rotary wing. In addition, a ducted fan configuration offers advantages such as high propulsive efficiency and high static thrust. An illustration of this concept is shown in Figure 1.

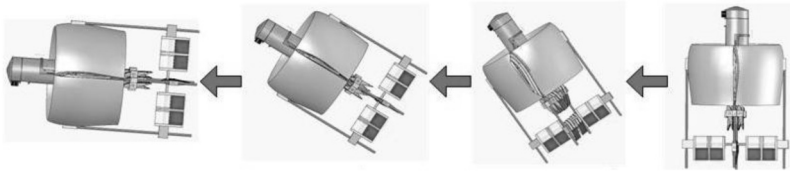


Figure 1: Various Attitudes of the Ducted-fan UAV between Hover and Cruise

Recently, AVID LLC[1, 2] has successfully designed and commissioned the ducted-fan UAV platforms in US Army for military applications. Nieuwstadt [3] has done the seminal work on the application of ducted-fans for UAV applications. Aurora Flight Sciences have come up with the unique design of the clandestine UAV called Goldeneye[4]. It is a ducted fan configuration with the control surfaces submerged in the prop-stream. The vehicle is claimed to have a good hover gust rejection response and transition performance as a result of its unique torsionally-decoupled outer wing panels. This phenomena is referred as aerodynamic-vectoring and detailed investigations are carried out by Maqsood and Go [5-7].

Ducted-fan UAVs are popular because they produce high static-thrust for a given diameter than the open propeller counterparts. Typical mission profile of such UAVs include maneuvers like vertical takeoff and landing, hover, efficient forward cruise and multiple transitions between hover and forward flight. The UAV is supposed to fly in closed cluttered terrains and is subjected to rough air patches and cross-winds. Due to the presence of large turbulent eddies created by buildings, hills, trees and other obstacles, the stable operation of such aircraft becomes more difficult. Across this velocity spectrum, the aircraft must have sufficient control authority to avoid such disturbances.

In this paper, a systematic improvement is carried out in the aerodynamic design of an existing platform (used as dynamics and control test-bed) at Nanyang

Technological University (NTU), Singapore. For this purpose, experimentation in the wind-tunnel facility is carried out. The baseline configuration is tested for hover as well as forward flight conditions. Explicit changes in the platform are made in hover such as propulsion system and associated control surfaces selection and positioning. For forward flight scenarios, wings of different aspect ratios are attached with the ducted fan and aerodynamic improvement is estimated. Finally, based on sequential analysis, a refined configuration is selected as a test-bench for future control and autonomous navigation studies.

Experimental Setup and Testing

Description of the Model

The front, top, side and oblique views of the baseline configuration of the UAV model are shown in Figure 2. It has a single propeller ducted-fan configuration, payload box in front and short wings. The wings of the UAV are hinged with the duct at quarter-chord length and can be rotated to the desired angle during the flight. The airfoil section for wings is also of the Eppler-180 class. The control surfaces are submerged in the slipstream aft of the duct. The maximum dimensions of the aircraft are 0.65 m axially and 0.5 m laterally. The duct has an Eppler-180 airfoil cross-section with the chord length of 0.145 m and inner diameter of 0.235 m. The diameter of the duct alone is defined as the ratio of inner diameter to chord length. Therefore, the aspect ratio of the duct alone is 1.62.

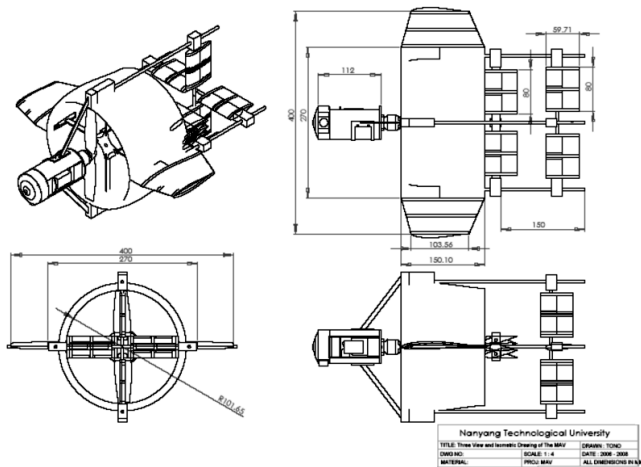


Figure 2: Top, Side, Front and Oblique Views of the Ducted-fan UAV

The zoomed view of the control surfaces arrangement aft of the duct is shown in Figure 3. It consists of six stators (three on each side), two rudder and two elevator surfaces respectively. The vertical and horizontal control surfaces have NACA-0018 airfoil sections and rectangular platforms. During the initial conceptual design, the stators were installed to cater for the counter-torque produced by the propeller. The slipstream effect is calculated based on Leishman [8] approximations for fan-tail design. The positioning of the elevator and rudder surfaces was carried out based on the preliminary investigations by Fleming [2] at AVID LLC.

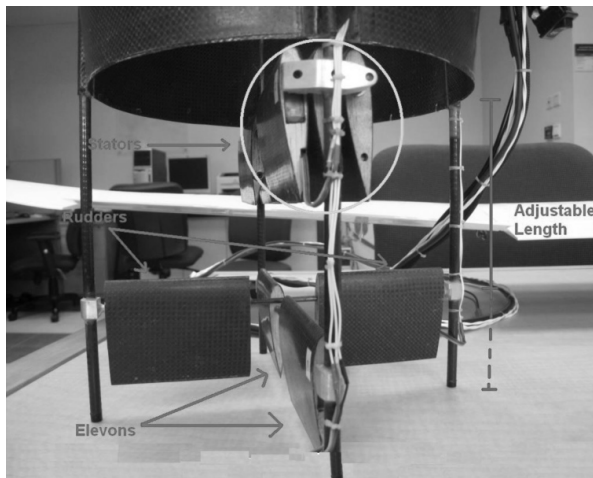


Figure 3: Existing Control Surface Distribution

Wind-Tunnel Setup

In order to predict the aerodynamic characteristics for various flight conditions, wind tunnel testing is carried out on the full scaled model of the original configuration. The model is constructed using Acrylic-Butadiene Styrene (ABS) material commonly used in lego blocks (Figure 4). The experimentation is carried out in a low-turbulence, closed-circuit wind tunnel at Nanyang Technological University (NTU). The operating speed of the wind tunnel ranges from 6 m/s to 90 m/s. The test section used is 2 meter long with a rectangular cross-sectional area of 0.78 m by 0.72 m. The model positioning system is of quadrant type and is equipped with a sting model support. It is capable of allowing the model to perform rotations in three axes, namely roll, pitch and yaw. The six component internal balance is used to measure lift, drag and pitching moment. The Data Acquisition, Reduction and Control System (DARCS) is based on National Instruments (NI) platform and Lab-View® based software.

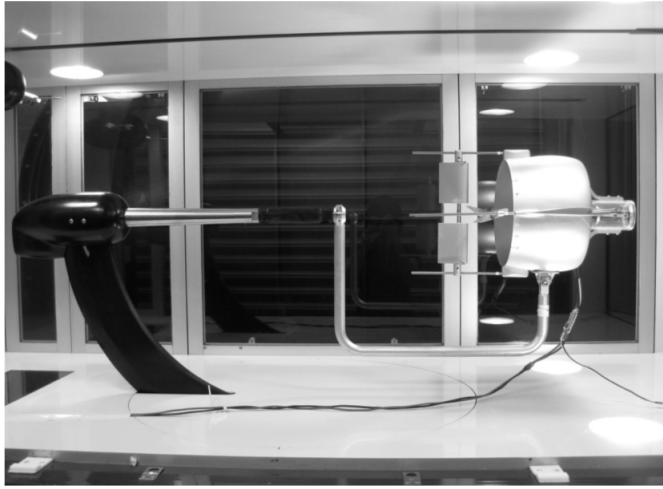


Figure 4: Mounting of the Ducted-fan UAV in the Wind-tunnel Test Section

Force and moment coefficients presented in this work have all been corrected for wind-tunnel blockage effects (solid blockage, wake blockage and streamline curvature) according to the techniques presented by Barlow [9]. The magnitude of the blockage effects increases with the increase in angle of attack. Generally, the magnitude of blockage corrections for most of the scenarios is less than 15%. The Reynolds number at which testing is carried out is approximately 0.15 million.

Propulsion System Setup

Beside the wind-tunnel facility and wind-tunnel model to be tested, the complete experimental setup is a combination of several electronic components. For the single-propeller configuration, Tahmazo® ER2822/1100 is used whereas, for the twin contra-rotating propeller system Himax® CR2816-1100 motor is used. The Electronic Speed Controller (ESC) is different for both configurations based on the recommendations by motor manufacturers. Pololu® serial 8-servo controller is used for the controlled actuation through MATLAB®. In this case, the RPM of the motors is controlled through computer using Simulink®. In order to power up the system with sustained current supplies, two power supplies are used: one for the motor and second for the servo controller. The servo controller can be powered through ordinary power supply as the current demand is quite low. The power supply used for the motor will be GW® Instek PSH-3630A, a single output 36V/30A 1080W programmable switching power supply with significantly low ripple noise. The control signal from a Personal

Computer (PC) to the ESC is sent through the Pololu® Serial 8 Servo Controller interface. The control signal from the PC can be varied from 0 to 255 bits. The revolution rate of the propeller is calibrated against the control signal through tachometer. To power this setup, a GW Instek PSH 3630A ground based DC source is used. The maximum power supplied to the both motors is 12 V and 10 A at any instant during testing. The schematic of the propulsion system setup for the experiment is shown in Figure 5.

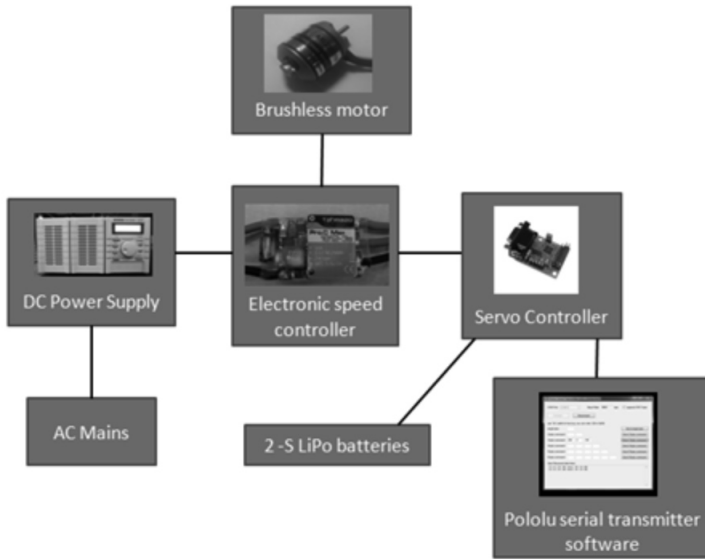


Figure 5: Schematic of the Propulsion System and Its Control

Hover Flight

Single Propeller Configuration

In this section, the effect of elevator effectiveness in the presence or absence of stators is evaluated for single propeller configuration. Beside that the effectiveness of stator itself is evaluated and an alternate configuration with the stators absent and elevators working as elevons is also evaluated.

Elevator Effectiveness

The effect of stators on the elevator effectiveness is shown in Figure 6. The gradient of this graph can be referred as stability derivative M_{δ_e} associated with

the control vector. It is observed that with the positive deflection of elevator, more pitch down moment can be generated and that is consistent with the standard axes rotation. It can be inferred that the absolute magnitude of M_{δ_e} is higher without stator presence. This clearly shows that there is a strong interference factor of stators on the elevator effectiveness. Generally a steeper slope is desired because with minimal control effort, higher moments may be generated. M_{δ_e} with stators is 0.235 kgf-m/rad and without stators is 0.271 kgf-m/rad . It is confirmed that the removal of stators in this configuration will increase the elevator control power as well as the control authority under cross-wind conditions.

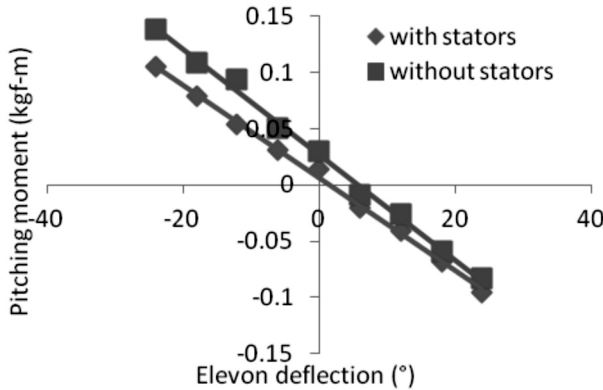


Figure 6: Pitching Moment Comparison (Effect of Stators)

The effect of position on the elevator effectiveness is evaluated in Figure 7 with the stators present. The positions are shown in terms of percentages of duct length. For example, the position of the leading edge of elevator just at the trailing edge of the duct is referred as 0% of duct length whereas, the original position of the elevator is 65.5% of duct length. It is observed that the trim elevator angle is 2° for the 65.5% duct length and 10° for the 115.2% duct length behind duct. Moreover, it is observed that the position of the elevators behind duct does not change the slope of the graph and therefore, it can be said that M_{δ_e} is independent of the position of elevators behind duct. It is also observed that as the distance is increased, higher deflection angle is required to trim the aircraft thereby indicating that there is a possible decrease in slipstream velocity.

Stator Effectiveness

The control effectiveness of the stators in countering the induced rolling moment from the single propeller configuration is studied in this section. The net rolling moment produced by the UAV at various RPM and stator deflections

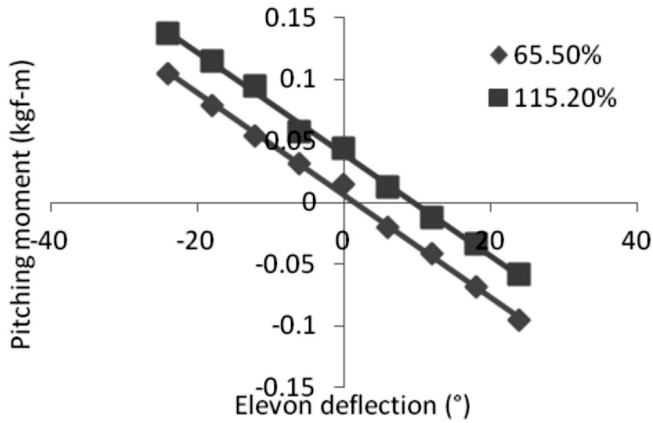


Figure 7: Pitching Moment Comparison (Effect of Elevators)

is shown in Figure 8. In addition to that, the net induced rolling moment in the absence of stators solely contributed by the single propeller is also plotted. It can be seen that the induced rolling moment is not counter-rotated by the stator deflection at various angles of stators deflection for all the RPM. The rolling moment experienced is therefore for a large amount and is nowhere near to zero and problem worsens near hover condition. Therefore, it can be concluded that the stators of the ducted fan UAV are not fulfilling its responsibility of

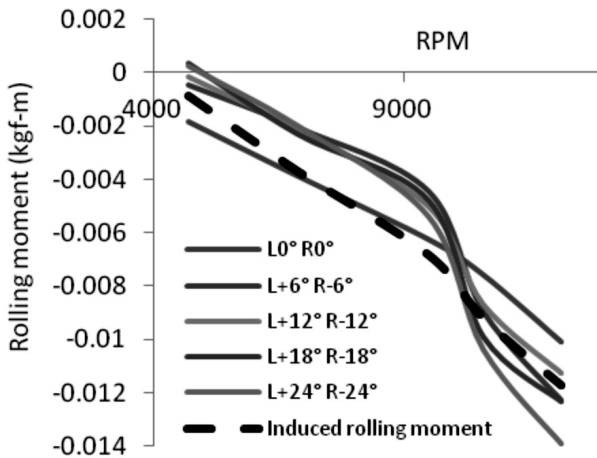


Figure 8: Control Effectiveness of Stators Against Induced Rolling Moment

counter-rotating the spiral air flow caused by the propeller of the motor and the insufficient control authority of the stators to counter the induced rolling moment can be deduced.

Elevons Effectiveness

After the realization of the fact that stators fail to counter the induced rolling moment, the next approach is adopted to remove the stators and use elevators as elevons. The effect of position on the differential deflection of the elevator is also evaluated. In Figure 9, the differential deflection of elevators (working as ailerons) is plotted against the net rolling moment of the UAV in hover condition. Moreover, the effect of position is also shown for three points behind duct. It can be clearly seen that none of the three trend pass through horizontal axis thereby clearly indicating that the trim angle cannot be achieved within the specified range. Therefore, it can be said that because of the significant amount of the torque generated by the single propeller configuration, stators as well as elevons have failed to provide roll trim condition. The position change is also insignificant for the remedy. A subsequent design strategy is to change the single propeller motor to contra-rotating twin propeller motor to overcome this discrepancy.

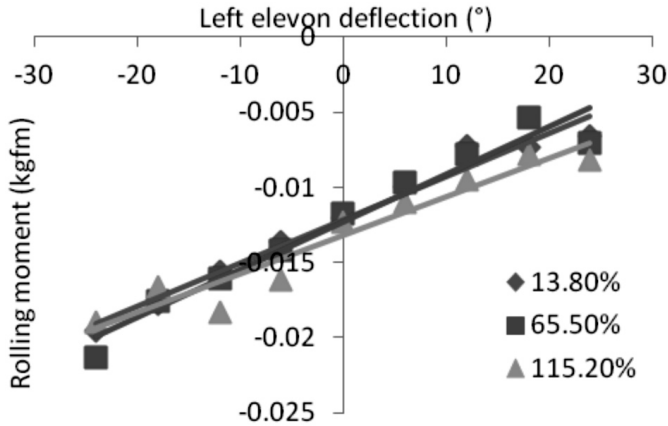


Figure 9: Rolling Moment Comparison (Position of Elevons)

Contra-Rotating Propeller Configuration

The effect of elevator positioning on the effectiveness of contra-rotating propeller configuration is analyzed in Figure 10. It can be observed that the pitching moment stability derivative M_{δ_e} is sensitive to the position of elevator in prop-

stream. The results reveal that M_{δ_e} starts to reduce as the elevators are located far downstream. The value of M_{δ_e} reduces by 30% as the position of elevators is moved from 17.9% to 115.2% of duct length inside prop-stream. This means that in order to trim the aircraft at higher angles, substantial amount of control effort is required if the position of the control surfaces is farthest from the duct trailing edge. Moreover, the difference between first two locations is relatively less as it clearly indicates that the prop-stream energy starts to reduce significantly after this position. Therefore, as a design rationale, it can be concluded that the elevators must be placed as near as possible to the propeller.

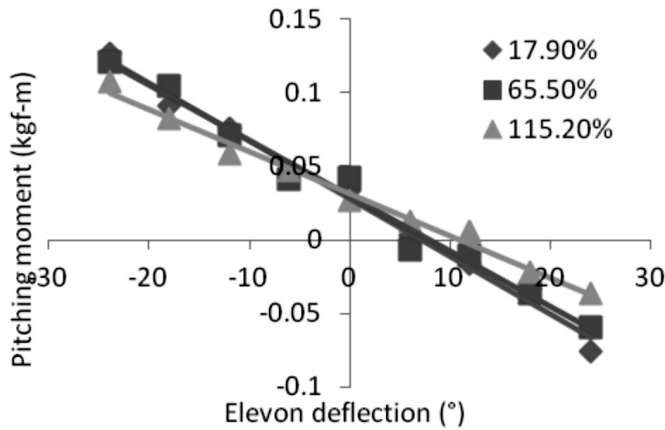


Figure 10: Pitching Moment Comparison (Position of Elevons)

Thrust Comparison

One of the key objectives of the study is to increase the thrust at reduced RPM so that with lesser current drawn, high thrust can be generated. The comparative analysis of thrust generation between single propeller and twin propeller is shown in Figure 11. It can be observed that the thrust produced by the twin propeller is greater than the single propeller across a certain RPM. Therefore, in order to fly the aircraft at hover position, the RPM required by the twin propeller is significantly less than its counterpart. The expansion of thrust envelope gives the leverage to the field operators to put additional payload in the form of sophisticated cameras for critical missions.

Rolling Moment Comparison

As discussed earlier, single propeller configuration does not have sufficient control effectiveness to remove induced roll rate because of propeller. For twin

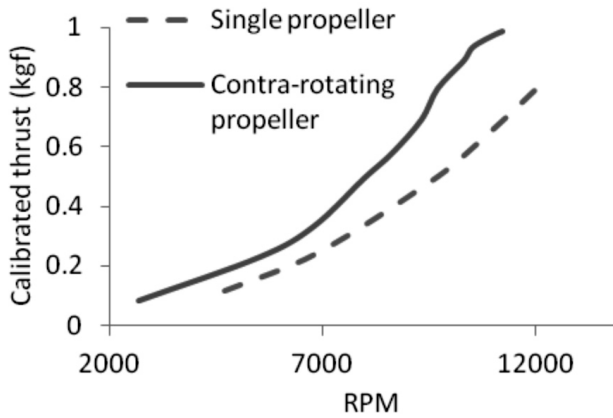


Figure 11: Thrust Comparison between Two Motor Configurations

propeller configuration, intuitively, this problem should be diminished. The comparison between rolling moments of the two different configurations is shown in Figure 12. The net rolling moment at a certain RPM is plotted and it can be clearly observed that at lower RPM, the twin propeller is generating no induced torque at all. However, at high RPM, there is a mild offset in resultant rolling moment but of negligible nature. There can be two techniques to cater for this minor offset. One of the techniques is to use the differential drive. This is more trivial and easy technique and can be done in the control design phase. Second technique is to resize the two propellers so that the net result for the static case is zero. This is more time demanding and is considered to be out of the scope of the paper.

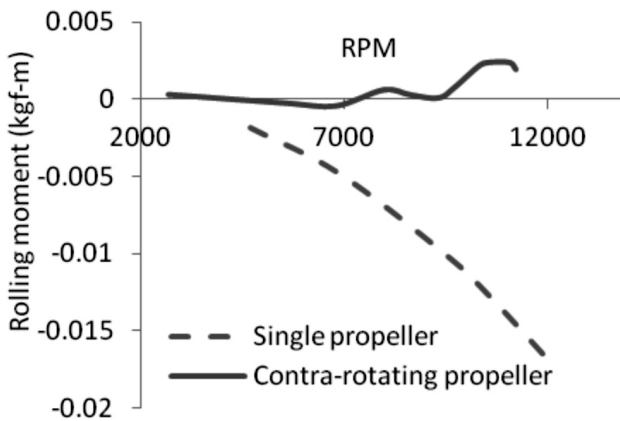


Figure 12: Rolling Moment Comparison between Two Motor Configurations

Slipstream Velocity Comparison

In this section slipstream velocity profile is studied for single and twin propeller configurations behind duct. The slipstream velocity profile of single propeller configuration at several locations is shown in Figure 13. The slipstream velocity distribution is shown at 13.8%, 65.5% and 115.2% duct length behind trailing edge of duct is plotted. Comparing the three profiles, it is apparent that a position of 13.8% duct length behind duct, the slipstream profile is in the process of buildup and is in pre-mature stage. The slipstream velocity varies drastically from 13.5 m/s to 28 m/s from 0 to 5.5 cm radius and then drops from 28 to 11 m/s from 5.5 to 7.5 cm radius. The profile trend at 13.8% and 65.5% duct length positions show in close agreement with Akturk [10] for ducted fan configurations.

The profile contour for 13.8% and 65.5% positions is almost similar and it can be said the slipstream profile is in the process of buildup and by the position 115.2%, the flow is fully matured and slipstream profile is more similar to theoretical shape. The significant decrease at the periphery of the duct shows a strong presence of shear layer and may be studied computationally in detail in future.

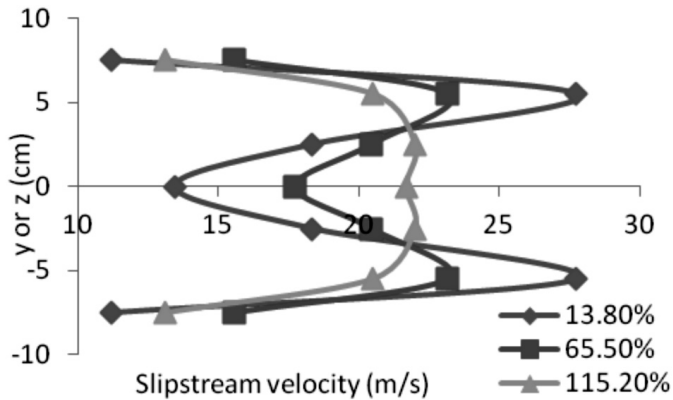


Figure 13: Slipstream Velocity behind Duct for Single Propeller Configuration

The slipstream velocity profile for twin propeller configuration follows similar trend of single propeller configuration and has not been discussed here explicitly for brevity. Figure 14 shows the comparison of average slipstream velocity aft of the trailing edge of the duct between single and twin propeller configurations. It can be seen that for all the positions of the control surfaces behind the duct, the slipstream velocity of the twin propeller configuration is higher than the slipstream velocity of the single propeller configuration.

Moreover, difference between average slipstream velocities for 13.8% and 65.5% duct-length behind duct are negligible for both configurations. The difference for single and twin propeller configurations is approximately 3.1% and 1.8% respectively thereby indicating that the difference is smaller for latter.

On the other hand, the average velocity comparison between 65.5% and 115.2% duct-length behind duct indicate the significant decrease. The difference for single and twin propeller configuration is approximately 6.1% and 6.3% respectively. Thus it can be inferred that the decrease in control power of the control surfaces for the single and twin propeller configurations is of the same extent.

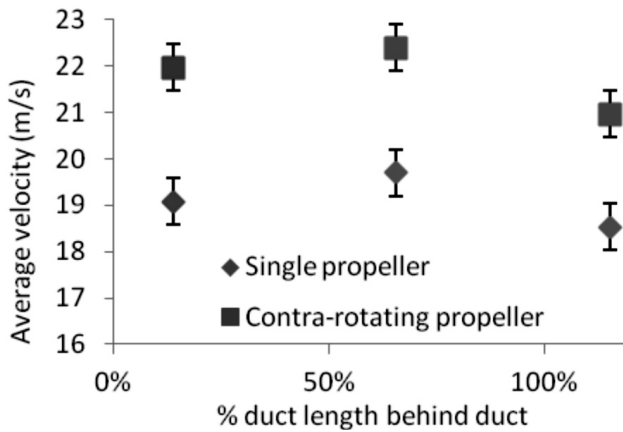


Figure 14: Slipstream Velocity Comparison between Two Motor Configurations

Based on the discussion above, it can be concluded that twin propeller configuration is better in terms of overall average velocity at all locations behind duct. It is obvious from the fact, that the two propellers will energize the slipstream velocity better than the single propeller of the same diameter. The study aimed at the improvement in the performance of a ducted fan UAV during hover flight. The control surfaces arrangement is very critical for hover mission segment. Since there is no free-stream velocity, control surfaces are energized by the prop-stream only. In cruise phase, free-stream presence is sufficient to generate control authority to execute agile maneuvers. So the final configuration consists of contra-rotating motor with elevators positioned just at the exit of the duct.

Final Optimized Ducted-Fan Configuration

The study aimed at the improvement in the performance of a ducted fan UAV during hover flight. The control surfaces arrangement is very critical for hover mission segment. Since there is no free-stream velocity, control surfaces are energized by the prop-stream only. In cruise phase, free-stream presence is sufficient to generate control authority to execute agile maneuvers. So the final configuration consists of contra-rotating motor with elevators positioned just at the exit of the duct.

Cruise Flight

The control surfaces arrangement for cruise flight is the same as of hover condition. The aerodynamic coefficients of the ducted-fan configuration in cruise mode are evaluated at the velocity of 15 m/s. Figure 15 shows coefficient of lift, drag and pitching moment. The trends are consistent with the literature. However, it should be noted that the coefficient of pitching moment is zero at zero angle of attack. This implies that the aircraft needs to be trimmed at some positive elevator deflection during horizontal cruise flight. This may be undesirable; however it can be circumvented by modifying the CG position. This task is envisioned as part of future work. Moreover, the pitching moment graph show $C_{M_0} < 0$ that satisfies the condition of static longitudinal stability at lower angles of attack. Beyond the angle of attack of 9° , the static longitudinal stability condition is reversed and therefore, a stability augmentation system may be required.

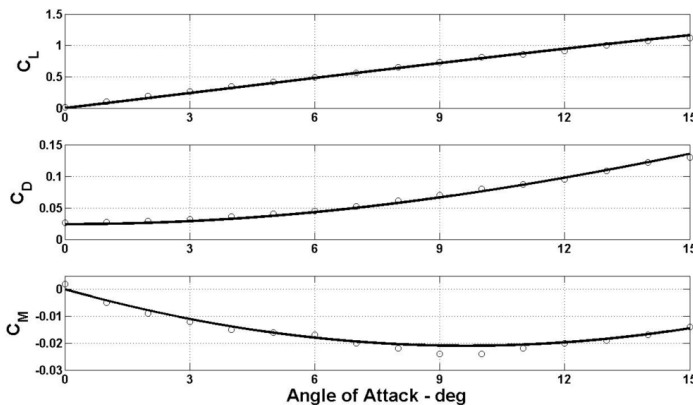


Figure 15: Coefficient of Lift, Drag and Moment of Ducted-Fan in Cruise

Duct-Wing Superimposition Studies

Effect of Aspect Ratio

In order to improve the lift characteristics of the UAV during cruise, wings of different aspect ratios can be attached to the duct. Therefore, three different configurations of aspect ratios 2.67, 3.72 and 4.42 are tested. The coefficient of lift for different aspect ratios is plotted in Figure 16. The coefficient of lift for the duct alone (aspect ratio = 1.62) is also plotted for comparison. Since the airfoil for the wing is Eppler-180, therefore, once the wings are attached with the duct, the zero lift coefficient becomes positive and increases with the aspect ratio. Moreover, the lift-curve slope also increases as the aspect ratio is increased. The stall angle of attack reduces with the increase in aspect ratio of the aircraft. Depending on the mission requirements and the payload capacity, wings of different aspect ratios can be attached to the aircraft.

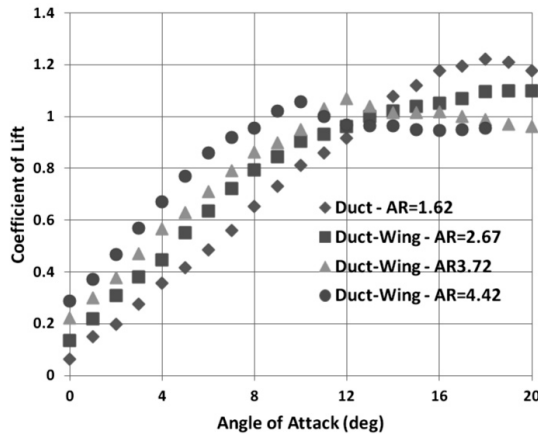


Figure 16: Lift Coefficient for Different Aspect Ratios of Duct-wing

Conclusion

The study aims at the improvement in performance of a ducted-fan UAV during hover and cruise. The effects of various configurations on the overall control effectiveness are discussed. Moreover, comparisons between single propeller and twin propeller configurations are drawn from various aspects such as the thrust and control power. It is concluded that for the single propeller configuration, the elevators are more effective once the stators are removed. Moreover, stators show inadequate control authority over roll moment. Therefore, the single propeller

configuration is replaced by twin propeller configuration which in return gives clean air to the elevator and rudder surfaces (in absence of stators) with high prop-stream velocity. Moreover, the trim roll moment can be achieved across the range of RPM. The change of motors has not increased the weight; in fact the removal of stators has reduced the overall weight of the vehicle. For the cruise mode, effect of wings of different aspect ratios is evaluated. Specifically, the lift properties improved significantly.

References

- [1] Ko, A., O.J. Ohanian, and P. Gelhausen. (2007). *Ducted Fan UAV Modeling and Simulation in Preliminary Design*. in *AIAA Modeling and Simulation Technologies Conference and Exhibit*. AIAA 2007-6375.
- [2] Fleming, J., T. Jones, W. Ng, P. Gelhausen, and D. Enns, (2003). *Improving Control System Effectiveness for Ducted Fan VTOL UAVs Operating in Crosswinds*. in *2nd AIAA "Unmanned Unlimited" Systems, Technologies and Operations*. San Diego, California: AIAA 2003-6514.
- [3] Nieuwstadt, M.J.V. and R.M. Murray, (1998). *Rapid Hover-to-Forward-Flight Transitions for a Thrust-Vectored Aircraft*. *Journal of Guidance, Control, and Dynamics*, 21(1): 93-100.
- [4] Schaefer, C.G. and L.J. Baskett, (2003). *GOLDENEYE: The Clandestine UAV*. in *2nd AIAA "Unmanned Unlimited" Systems, Technologies, and Operations*. San Diego, California: AIAA 2003-6634.
- [5] Maqsood, A. and T.H. Go, (2011). *Optimization of Transition Maneuvers Through Aerodynamic Vectoring*. *Aerospace Science and Technology*.
- [6] Maqsood, A. and T.H. Go, (2011). *Multiple Time Scales Analysis of Aircraft Longitudinal Dynamics with Aerodynamic Vectoring*. *Nonlinear Dynamics*.
- [7] Maqsood, A. and T.H. Go, (2010). *Optimization of Hover-to-Cruise Transition Maneuver Using Variable-Incidence Wing*. *Journal of Aircraft*, 47(3): 1060-1064.
- [8] Leishman, J.G., (2006). *Principles of Helicopter Aerodynamics*. Second ed. Cambridge Aerospace Series. Cambridge University Press.

- [9] Barlow, J.B. (1999). *Low-speed Wind Tunnel Testing*. Wiley.
- [10] Akturk, A., A. Shavalikul, and C. Camci. (2009). *PIV Measurements and Computational Study of a 5-Inch Ducted Fan for V/STOL UAV Applications*. in *47th AIAA Aerospace Sciences Meeting and Exhibit*. Orlando, Florida: AIAA.